N, N'-(1,2-Pheneylene) bis (3,4,5-Trihudroxybenzamide) as Bioactive Ligand Synthesis, Analytical and Anti-Microbial Studies

Esraa O. Ahmed[1], Abdou S. El-Tabl[2], Eman A. Mohamed[2],

Islam M. I. Moustafa[1*]

[1]Department of Chemistry, University of Banha, Banha, Egypt

[2]Department of Chemistry, University of Menofia, Shibin El Kom, Egypt

ABSTRACT

The synthesis and characterization of some metal complexes with new polyhydroxyl amide ligand derived from Gallic acid viz: N, N'-(1,2-phenylene) bis (3,4,5-trihydroxy benzamide), expected to have biological activity, had been synthesized and characterized by different spectroscopic and physical techniques. In solution, the study focused on the formation of Mn^{2+}, Fe^{3+}, Ni^{2+}, Cu^{2+} and Zn^{2+} complexes with the newly prepared ligand. Firstly, the stoichiometry of the complexes was determined by conductometric titration then the proton-ligand ionization constants (log K_n^H) and metal-ligand stability constants (log β_n^M) were determined by potentiometric titration. The former proved the formation of 1:1 and 2:1 (L:M) complexes while the stability constants were found to be dependent on the effective charge (e/r) ratio of the metal ion. In solid state, metal complexes with different metal ions (Mn^{2+}, Fe^{3+}, Ni^{2+}, Cu^{2+} Zn^{2+}, Ca^{2+} and Pb^{2+}) and different anions (SO_4^{2-}, AcO^-) had been successfully prepared and characterized by elemental and thermal analysis, mass spectra, IR, ^1HNMR, ESR and TEM techniques. The biological activity of the prepared complexes towards two Gram positive bacterial species (Staphylococcus aureus and Bacillus subtilis), two Gram negative bacterial species (Escherichia coli, Proteus vulgaris), one filamentous fungus (Aspergillus fumigatus) and one yeast species (Candida albicans) was studied using the modified well diffusion method. The optained results showed higher activities of the solid complexes compared to that of the free ligand.

Keywords: Hydroxyl amide ligand; Gallic acid; Transition metal complexes; Conductometry; Potentiometry; Biological activity

INTRODUCTION

Gallic acid (3,4,5-trihydroxybenzoic acid) is one of the most abundant phenolic acids in the plant kingdom. It and many of its derivatives have extensive application in the food and pharmaceutical industries and can inhibit the oxidation and rancidity of oils and fats due to their free radical scavenging and antioxidant nature [1]. Many scientific researches on the biological and pharmacological activities of these phytochemicals were reported with emphasis on antioxidant, antimicrobial, anti-inflammatory, anticancer, cardio protective, gastro protective, and neuroprotective effects [2-6]. These compounds can disrupt the integrity of the cell membrane in both Gram positive and Gram negative bacteria and change the charge, hydrophobicity, and membrane permeability of *Campylobacter jejune* then elevate the antibiotic accumulation in the microorganism [7-10]. Gallic acid can interfere with the Chemo Dynamic Therapy (CDT) provides a new treatment strategy for tumor cells. A variety of CDT agents have been designed by taking advantage of the catalytic property of transition metals, e.g., Fe, Cu, and Mn. Among those nano substrates, Cu-based CDT agents are obviously superior to the other transition metal-based counterparts [11]. Metal complexes derived from bioactive compounds (Gallic acid and others) are being explored for antimicrobial actions and potentially are applicable to provide effective and nontoxic drug candidates having preferred and improved pharmacological activity [12-16]. It should be noted that the presence of metal ions in biological fluids could have a significant effect on the therapeutic action of such organic compounds [17]. Although there are many methods available to study the stability of metal-ligand complexes, the potentiometric method had been used extensively in many branches of solution chemistry and is most frequently used for the study of binary and ternary complexes of transition metals with molecules of biological and pharmaceutical interest [18,19]. In the present work, and in continuation of our study, we provide the synthesis and characterization of Mn^{2+}, Fe^{2+}, Ni^{2+}, Cu^{2+}, Zn^{2+}, pb^{2+} and Ca (II) complexes with new polyhydroxyl amide ligand derived from Gallic acid. The stoichiometry and stability constants of the complexes are determined in solution by conductometric and potentiometric titrations. The biological activity towards some bacteria, fungi and yeast were also studied.

MATERIALS AND METHODS

All chemicals used in the present study were of higher-grade Merck or Alderich and were used as received. Second distilled water was used whenever water is necessary. The organic polyhydroxyl amide ligand was prepared by esterification of Gallic acid with ethyl alcohol and condensation with o-phenelynediamine (Figure 1). Solid complexes were prepared by refluxing of metal ion salt (in least amount of ethanol) with ethanolic ligand solution in molar ratio 1:1 or 2:1 (L:M) for about 6 hrs. All techniques and instruments used for characterization of metal complexes are as described in our previous works [20,21].

Conductometric titration

It was carried out, using YSI Model 32 conductance meter, by titrating 50 mL of ligand solution (10^{-2} M) with the metal ion solution (10^{-3} M) added from micro burette with mechanical stirring after the addition of each increment of

Citation: Moustafa IMI, et al. 2024. N, N'-(1,2-Pheneylene) bis (3,4,5-Trihudroxybenzamide) as Bioactive Ligand; Synthesis, Analytical and Anti-Microbial Studies. J. Chem Pharm. Res. 16:170.

Moustafa IMI, et al.   ***J. Chem. Pharm. Res., 2024, 16(7):1-16***

the titrant. Correction for the dilution effect on the measured conductance was performed by multiplying its value by the factor $(V_o + V_1/V_1)$ where V_o is the original volume of the solution (50.0 mL) and V_1 is the volume of the titrant. The corrected conductance (in μ Mohs) is then plotted as a function of the molar ratio (ligand/metal).
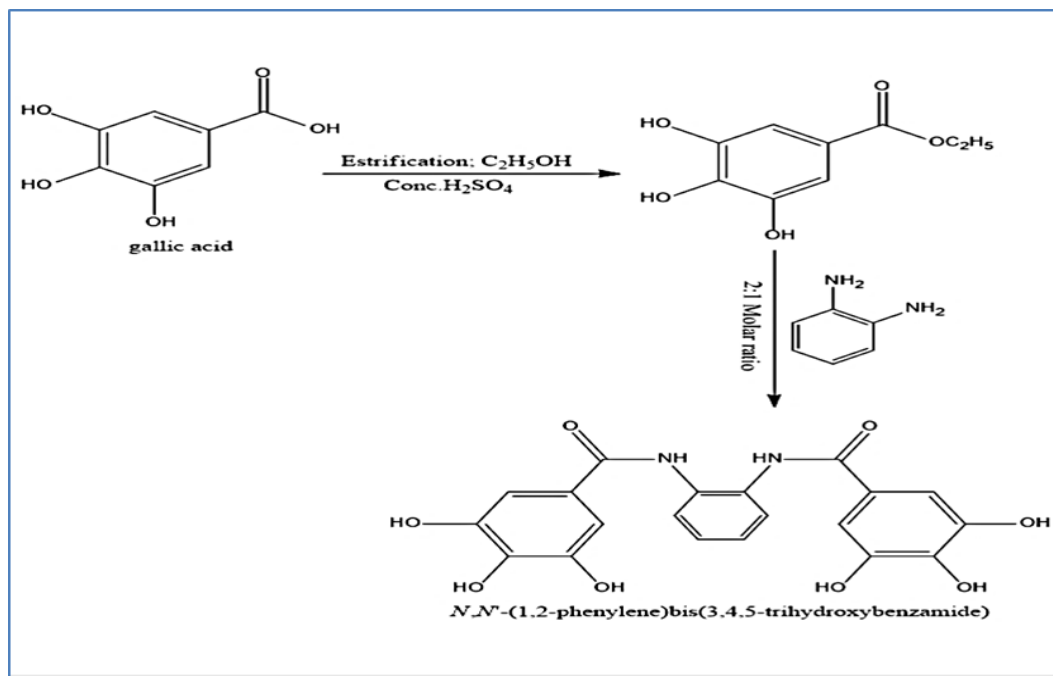

Figure 1: Gallic acid with ethyl alcohol and condensation with o-phenelynediamine.

Potentiometric titration

The following solutions were prepared:

(A): 5.0 mL of 0.1 M HCl and 5.0 mL of 1.0 M NaCl.

(B): Mixture (A) + 25 mL of 0.001 M ligand (in ethanol).

(C): Mixture (B) + 2.0 mL of 0.0025 M metal ion solution.

Each solution mixture was completed to 50.0 mL using ethanol and bi-distilled water so as to obtain 40% by volume ethanol. Each mixture was then titrated against 0.02 M NaOH solution containing the same percent of ethanol using an automatic micro burette with constant stirring.

Antimicrobial activity assay

The antimicrobial effect was tested against *Staphylo-coccus aureus* and *Bacillus subtilis* as Gram positive, *Escherichia coli* and *Proteus vulgaris* as Gram negative bacterial species in addition to one filamentous fungus; *Aspergillus fumigatus* and one yeast species; *Candida albicans* using a modified well diffusion method [22]. Briefly, samples are incubated at $37°C$ for 18-24 hours and are placed in the center of nutrient agar plates which have been inoculated with the test bacteria. The evaluation of this test is based on the level of growth both under and around the sample. The area of no growth is known as a "Zone of inhibition" or "Clear zone" which is proportional to

the inhibitory action of the investigated compound [23]. The resulting inhibition zone diameters were measured in millimeters and used as criterion for the antimicrobial activity. Solvent controls (DMSO) were included in every experiment as negative control. Positive controls were also performed using gentamycin as standard antibacterial drugs and the ketoconazole as standard antifungal drug. The lowest concentration showing complete inhibition of growth was recorded as the MIC of the respective sample [24].

RESULTS AND DISCUSSION

Part A: Studies on the metal complexes in solutions

In this part, the possibility of complex formation between ligand and Mn^{2+}, Fe^{3+}, Ni^{2+}, Cu^{2+} and Zn^{2+} metal ions in solution are discussed. The stoichiometry of the complexes formed was studied by conductometric titration while the proton-ligand stability constant, ($\log K_n^H$), of the free ligands and the metal-ligand formation constants, ($\log \beta_n^M$), of the complexes were determined by potentiometric titration.

Conductometric titration: The stoichiometry of the complexes formed between Mn^{2+}, Fe^{3+}, Ni^{2+}, Cu^{2+} and Zn^{2+} and the ligand under study is determined by conductometric titration. In the present work, the common behavior of the conductance-molar ratio plots is the increase in conductance with increasing volume of titrant (Figure 2). Although the ligand solution has negligible conductance, its addition to the metal ion solution caused a continuous increase in the conductance. The slopes of equivalent-conductivity plots for all ligand-metal ions mixtures showed significant changes when the mole ratio (C_L:C_M) was about 1:1 and 2:1; thus indicating the formation of a relatively stable 1:1 and 2:1 complexes (L:M) between Mn^+ and the ligand (Figure 2).
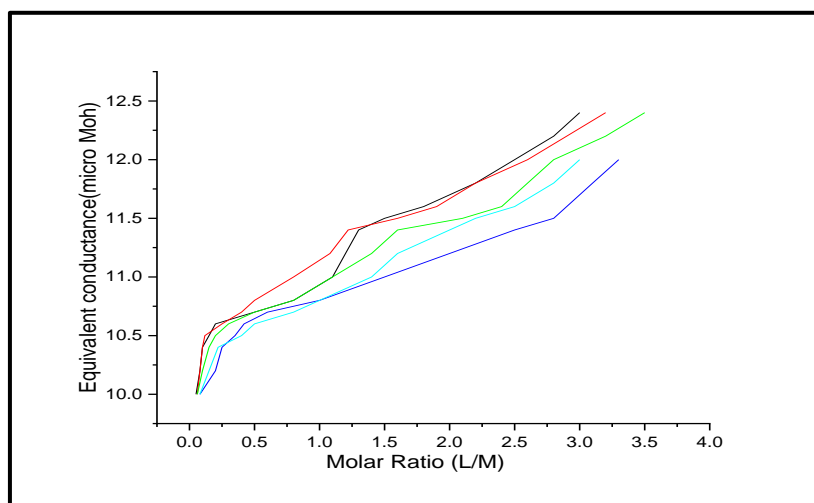

Figure 2: Conductometric titration of ligand (HL) with, Mn^{2+}, Fe^{3+}, Ni^{2+}, Cu^{2+} and Zn^{2+}. Note: (——): Mn (II); (——): Fe (III); (——): Ni (II); (——): Cu (II); (——): Zn (II).

Potentiometric titration: The potentiometric titrations were performed in presence of acid mixture (A) as medium consisting of 0.1 M HCl and 1.0 M NaCl as recommended by Bjerrum [25]. Mixture (A) was mixed with the chelating ligand (HL) of concentration of 1.0×10^{-3} M called mixture (B). Mixture (B) was mixed with different metal ions of concentration 2.5×10^{-3} M called C_1, C_2, C_3, C_4 and C_5 for Mn^{2+}, Fe^{3+}, Ni^{2+}, Cu^{2+} and Zn^{2+} ions respectively. In all mixtures A, B or C_n, absolute ethanol of 40% (v/v) is enough to keep the components of the mixture in soluble state. These mixtures were then titrated with 0.02 M NaOH freed from carbonate containing also 40% (v/v) ethanol to keep the ratio of ethanol in the titration vessel constant. The potentiometric titration curves of the mixtures are shown in Figure 3. These curves are S-shaped with a sharp jump in mixtures (A) and (B) but relatively smooth curves are obtained with mixtures C_n which contain the metal ions. The end points for the titration of the mixtures increase in the order A< B< C_n (Figure 3).
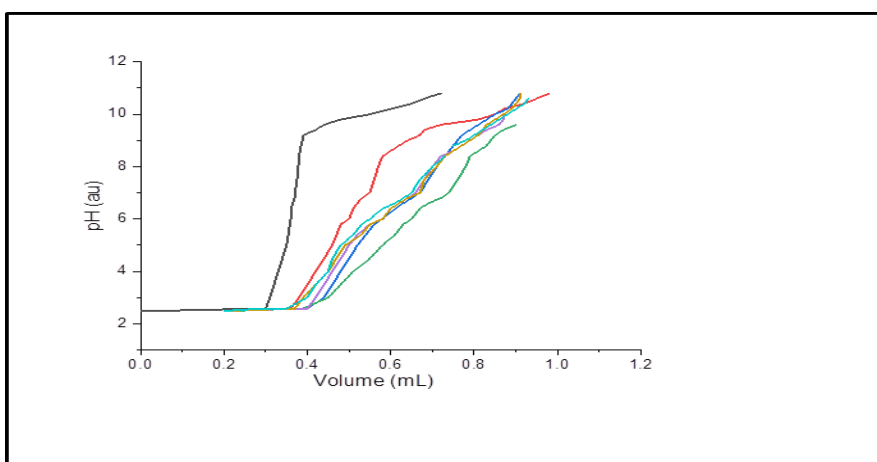

Figure 3: Potentiometric titration of Ligand (HL) in presence of Mn^{2+}, Fe^{3+}, Ni^{2+}, Cu^{2+}.and Zn^{2+}. Note: (▬): Acid Mix. (A); (▬): Mix. (B); (—): Mn^{2+}; (—): Fe^{3+}; (—): Ni^{2+}; (—): Cu^{2+}; (—): Zn^{2+}.

The average number of protons associated with the reagent molecule (n'_A) is determined at different pH values using the relation:

$$n'_{A=Y+\frac{(V_1-V_2)(N^o+E^o)}{(V^o+V_1)(TC_{Lo})}} \tag{1}$$

Where V_1 and V_2 the volumes of NaOH required to reach the same pH in the titration curve of acid mixture and the chelating drug, respectively, V^o the initial volume (50 mL), TC_{Lo} the total concentration of the drug, Y the total number of dissociable protons attached to the drug, N^o the normality of NaOH solution and E^o the initial concentration of the free acid. The values of n'_A are plotted against pH and the value of proton-ligand stability constants K_n^H is calculated by interpolation at half n'_A integrals (Figure 4).

To determine the values of stepwise formation constants of the complexes formed between metal ions and the ligand, the average number of ligand molecules attached per metal ions (n') and free ligand exponent (PL) are calculated using the equations:

$$n' = \frac{(V_2 - V_3)(N^O + E^O)}{(V^O + V_1) \, n'A (TC_{Mo})} \tag{2}$$

$$Pl = \log \frac{\sum_{n=0}^{n=j} \beta_n^H \left(\frac{1}{antilog\ pH}\right)^n}{(TC_{Lo} - n'TC_{Mo})} \times \frac{V^O + V3}{Vo} \tag{3}$$

Where TC_{Mo} the total concentration of metal ion presents in solution, β_n^H the overall stability constant, V_1, V_2 and V_3 are the volumes of NaOH required to reach the same pH in titration curves in acid mixture, organic ligand and the complex respectively. On plotting the values of n' against PL and interpolating at the half-integrals, the stepwise stability constants of the complexes can be evaluated (Figure 5).
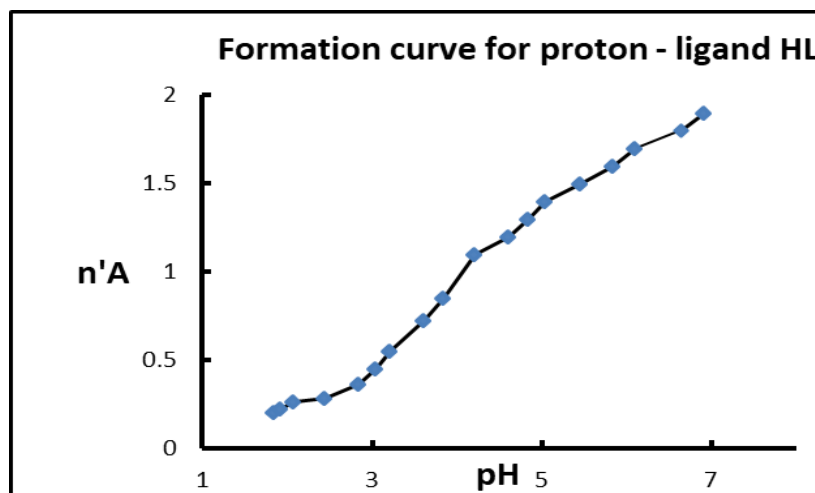

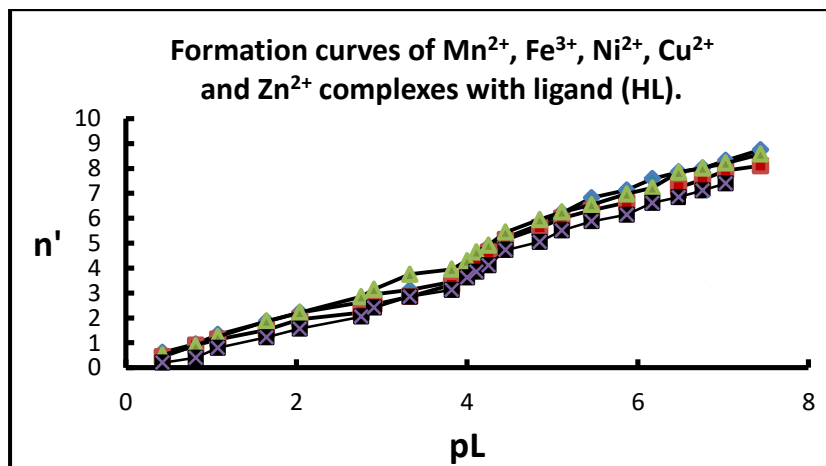**Figure 4: Formation curve of proton Ligand (HL).**

Figure 5: Formation curves of Mn^{2+}, Fe^{3+}, Ni^{2+}, Cu^{2+} and Zn^{2+} complexes with ligand (HL).

Note: (⬤─): Fe^{3+}; (─■─): Ni^{2+}.

The values of log K_n^H and log K_n^f gathered from potentiometric titration along with the effective charge (e/r) values are listed in Table 1.

Table 1: Proton-reagent stability (log K_n^H) and stepwise formation (log K_n^f) constants of Mn^{2+}, Fe^{3+}, Ni^{2+}, Cu^{2+} and Zn^{2+} complexes with ligand (HL).

Complex	logK_n^H	Step-wise formation constants; logK_n^f				
		Mn^{2+}	Fe^{3+}	Ni^{2+}	Cu^{2+}	Zn^{2+}
		(e/r)	(e/r)	(e/r)	(e/r)	(e/r)
HL	logK_1^H=3.1	4.11	4.64	4.22	4.52	4.31
	logK_2^H=5.5	0.026	0.043	0.026	0.029	0.023

Part B: Studies on the metal complexes in solid state

All the prepared complexes are nonhygroscopic, having different colours and of high melting points ($\geq 180^{\circ}C$). Elemental analysis measurements showed satisfactory agreement between the proposed and obtained formulae, while molar conductance values indicate their nonionic nature except those prepared from copper sulfate, lead sulfate (Table 2).

Table 2: Analytical and physical data of ligand (HL) and its metal complexes.

No.	Tentative formula	FW	M.P ($^{\circ}C$)	Anal./Found (Calc.) (%)					Conductivity Λ
				C	H	N	S	M	
HL	$C_{20}H_{16}N_2O_8$	412	240	58.47 (58.25)	4.15 (3.91)	7.07 (6.79)	-	-	-
I	((HL)Mn (OAc)$_2$(H$_2$O)$_2$).2H$_2$O $C_{24}H_{26}MnN_2O_{14}$	621	180	46.39 (46.15)	4.22 (4.2)	4.51 (4.4)	-	8.84	13.5
II	((HL) Ni (NO$_3$)$_2$ (H$_2$O)$_2$).2H$_2$O $C_{20}H_{20}N_4NiO_{16}$	631	210	38.42 (38.06)	3.05 (3.19)	9.17 (8.88)	-	9.3	14
III	((HL)Cu (OAc)$_2$(H$_2$O)$_2$).2H$_2$O $C_{24}H_{26}CuN_2O_{14}$	630	220	47.9 (45.75)	4.18 (4.16)	4.86 (4.45)	-	10.09	11.7
IV	((HL)Cu (SO$_4$) (H$_2$O)$_3$).2H$_2$O $C_{20}H_{22}CuN_2O_{15}S$	625	301	38.75 (38.37)	3.4 (3.54)	4.75 (4.47)	5.23 (5.1)	10.15	48
V	((HL)$_2$Ni (OAc)$_2$) .3H$_2$O $C_{44}H_{38}N_4NiO_{20}$	1001	250	53.2 (53.77)	3.62 (3.82)	5.89 (5.59)	-	5.86	13
VI	((HL)$_2$Cu (OAc)$_2$) .3H$_2$O $C_{45}H_{42}CuN_4O_{20}$	1022	320	52.87 (52.94)	4.14 (4.17)	5.48 (5.36)	-	6.22	11.5
VII	((HL)$_2$Zn (SO$_4$) (H$_2$O)).2H$_2$O $C_{40}H_{34}N_4O_{21}SZn$	1004	300	47.27 (47.84)	3.18 (3.41)	5.81 (5.58)	3.34 (3.2)	6.51	14.5

Citation: Moustafa IMI, et al. 2024. N, N'-(1,2-Pheneylene) bis (3,4,5-Trihudroxybenzamide) as Bioactive Ligand; Synthesis, Analytical and Anti-Microbial Studies. J. Chem Pharm. Res. 16:170.

Moustafa IMI, et al.   ***J. Chem. Pharm. Res., 2024, 16(7):1-16***

VIII	((HL)Ca (OAc)$_2$(H$_2$O)$_2$) 3H$_2$O	606	200	47.52	4.32	4.62	-	6.61	7
	C$_{24}$H$_{26}$CaN$_2$O$_{14}$			(47.45)	(4.25)	(4.55)			
IX	((HL)Ca (Cl)$_2$ (H$_2$O)$_2$).2H$_2$O	575	190	43.83	4.2	4.87	-	6.97	9.5
	C$_{21}$H$_{24}$CaCl$_2$N$_2$O$_{10}$			-43.75	-4.18	-4.77			
X	((HL)Pb (SO$_4$) (H$_2$O)$_3$).2H2O	769	210	31.21	2.88	3.64	4.17	26.92	30
	C$_{20}$H$_{22}$N$_2$O$_{15}$PbS			-31.19	-2.85	-3.6	-4.1		

Thermal analysis

The thermo gravimetrical behavior of some selected solid complexes is studied as further support for chemical structure. From the TG curves percent of physically adsorbed and coordinated water molecules were detected and the percent of metal ion in complexes was calculated from the percent of metallic residue remained after complete degradation. Table 3 summarizes the sequence and assignment of degradation steps and show representative thermo gram (Table 3), (Figure 6).

Table 3: Thermal analysis data for some metal complexes.

Complex	Temp. ($^\circ$C)	% Wt. loss	Assignment
III	44.27	57.317	Loss of (H$_2$O) hydrated water molecules.
	430.58	20.065	Loss of (H$_2$O) coordinated water molecules.
	666.31	12.686	Beginning decomposition with evolution of N$_2$ and CO$_2$
			Final decomposition of complex leading to CuO
IV	47.55	23.256	Loss of (H$_2$O) hydrated water molecules.
	322.9	45.361	Loss of (H$_2$O) coordinated water molecules.
	567.06	25.907	Beginning decomposition with evolution of N$_2$ and CO$_2$
			Final decomposition of complex leading to CuO
VIII	42.39	12.687	Loss of (H$_2$O) hydrated water molecules.
	235.22	15.664	Loss of (H$_2$O) coordinated water molecules.
	313.01	31.615	Beginning decomposition with evolution of N$_2$and CO$_2$
	605.28	29.273	Final decomposition of complex leading to CaO
IX	42.11	16.04	Loss of (H$_2$O) hydrated water molecules.
	333.45	54.15	Loss of (H$_2$O) coordinated water molecules.
	580.78	21.772	Beginning decomposition with evolution of N$_2$ and CO$_2$
			Final decomposition of complex leading to CaO

Citation: *Moustafa IMI, et al. 2024. N, N'-(1,2-Pheneylene) bis (3,4,5-Trihudroxybenzamide) as Bioactive Ligand; Synthesis, Analytical and Anti-Microbial Studies. J. Chem Pharm. Res. 16:170.*

Moustafa IMI, et al.   *J. Chem. Pharm. Res., 2024, 16(7):1-16*
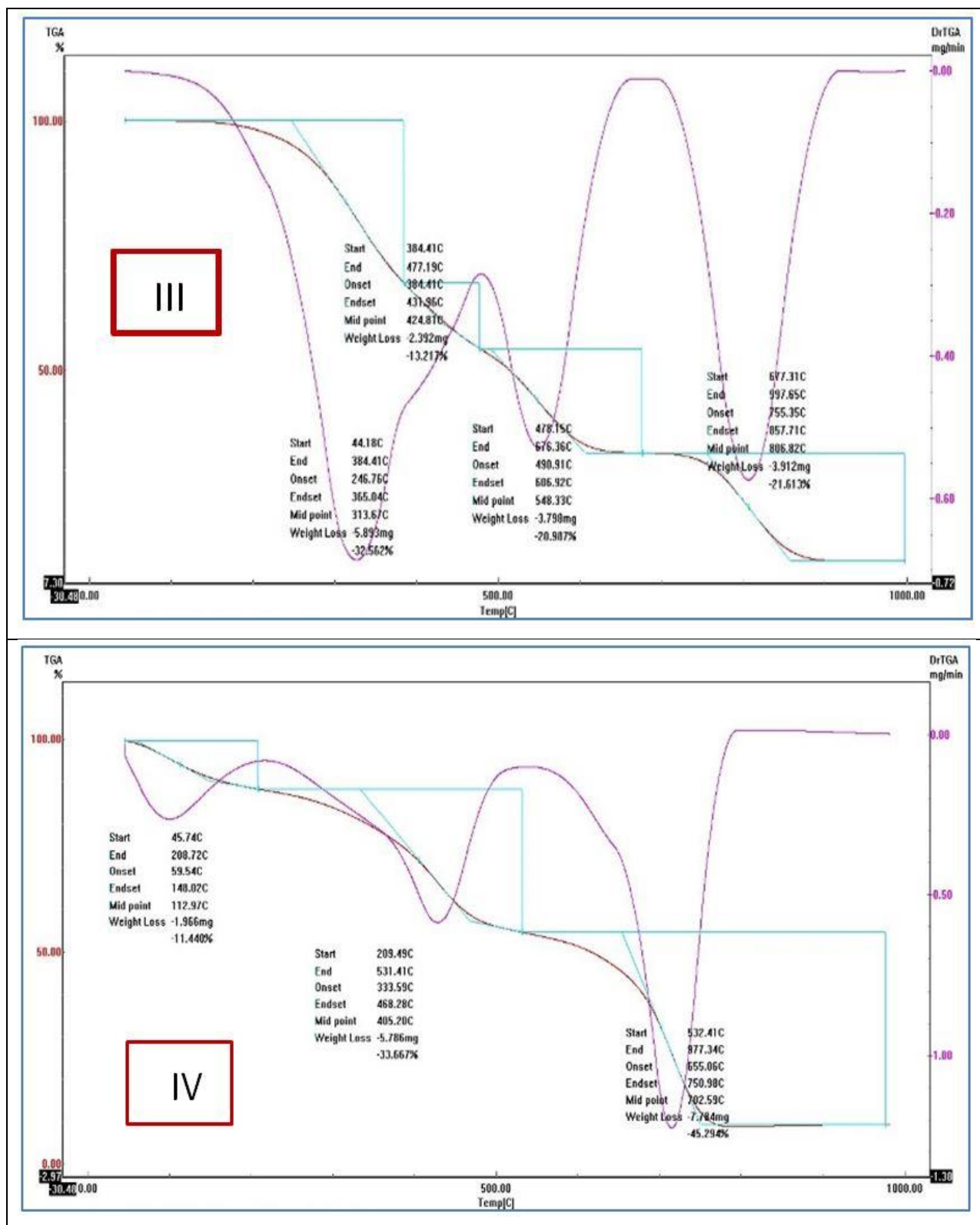

Figure 6: TGA thermal charts of complexes (III) and (IV).

Infrared spectra

To through light on the mode of bonding and functional groups participating in complex formation, the IR spectra of the solid complexes were compared to that of the free ligand using KBr disc technique. IR spectrum of the ligand (HL) showed broad band located at 3442 cm^{-1} and weak band at 3290 cm^{-1} due to the stretching vibrations of intra-molecular hydrogen bonded OH groups and the stretching vibration of NH_2 groups, respectively [26]. The latter band is strongly shifted to lower frequency in the spectra of complexes indicating its contribution in coordinate bond formation. On the other hand, the strong band present at 1604 cm^{-1} in the spectrum of the free ligand due to the υ (C═O) amide is, more or less, unaffected on the spectra of the solid complexes indicated that this group is not involved in the coordination to the metal ion. A new set of two bands located at 432-635 cm^{-1} and 533-750 cm^{-1} appeared in the spectra of solid complexes and were assigned to $\upsilon_{(M-N)}$ and $\upsilon_{(M-O)}$, respectively. Other frequencies (cm^1) of different anions of metal salts are cited in (Table 4).

Table 4: IR Frequencies (cm^{-1}) of some important band the ligand (HL) and its metal complexes.

Complex	$\nu_{(H2O)}$	$\nu_{(OH)}$	Y_{NH2}	δ_{OH}	$\nu_{(OAc/SO4/NO3)}$	$\nu_{(M-O)}$	$\upsilon_{(M-N)}$
HL	-	3442	3418	1385	-	-	-
I	3439	3481	3143	1319	1384, 1274	573	459
II	3520	3402	3150	1457	742	556	424
III	3679	3399	3257	1325	1400, 1325	750	635
IV	3678	3448	3141	1566	1394, 1277,667	550	458
V	3510	3450	3270	1504	1382,1311,882	590	452
VI	3452	3384	3175	1225	1,40,51,225	612	419
VII	3450	3415	3275	1459	1,27,71,107	544	458
VIII	3473	3430	3107	1272	1,45,61,425	586	461
IX	3471	3447	3068	1386	-	669	611
X	3505	3428	3205	1240	1035,879, 859	433	418

Mass spectra

In combination with elemental and thermal analysis, mass spectra of the solid complexes were measured to ascertain their chemical structure. The technique is accurate and give confidential results. The molecular peaks (m/z; amu) of different fragments are cited with assignment in (Table 5).

Table 5: Mass spectral data (Molecular ion peak; m/z; amu) for some selected complexes.

Complex	Mole. ion peak m/z	Assignment	Mole. ion peak m/z	Assignment
Free ligand	76	C_6H_4,	335	$C_{14}H_{11}O_8N_2$
	181	$C_{12}H_5O_2$	374	$C_{17}H_{16}O_8N_2$
	304	$C_{14}H_8O_8$	400	$C_{19}H_{16}O_8N_2$
			412	$C_{20}H_{16}O_8N_2$ (F.Wt
((HL)Mn (OAc)$_2$(H$_2$O)$_2$).2H2O (I)	171	$C_6H_7O_4N_2$, $C_{10}H_{13}O_6N_2Mn$ $C_{10}H_{16}O_6N_2Mn$ $C_{14}H_{21}O_7N_2Mn$	418	$C_{15}H_{23}O_8N_2Mn$, $C_{21}H_{23}O_9N_2Mn$, $C_{22}H_{25}O_{11}N_2Mn$, $C_{24}H_{25}O_{13}N_2Mn$ $C_{24}H_{26}O_{14}N_2Mn$
	257		505	
	319		552	
	388		604	
			621	
((HL)Cu(OAc)2 (H2O)2).2H2O (III)	444	$C_{14}H_9O_{11}N_2Cu$, $C_{14}H_{14}O_{11}N_2Cu$ $C_{16}H_{16}O_{11}N_2Cu$ $C_{17}H_{16}O_{11}N_2Cu$	535	$C_{18}H_{20}O_{13}N_2Cu$, $C_{20}H_{26}O_{14}N_2Cu$ $C_{24}H_{26}O_{14}N_2Cu$
	449		581	
	475		629	
	487			
((HL)Cu (SO$_4$) (H2O)3).2H2O (IV)	192	$C_4H_4O_5N_2S$, $C_6H_{10}O_5N_2S$, $C_7H_{12}O_5N_2SCu$ $C_7H_{15}O_6N_2SCu$	398	$C_{11}H_{15}O_8N_2SCu$,
	222		433	C11H18O10N2SCu,
	299		519	C14H20O13N2SCu,
	318		601	C18H22O15N2SCu,
			626	C20H22O15N2SCu
((HL)$_2$Ni (OAc)$_2$) .3H$_2$O (V)	276	$C_7H_6O_9N_3$, $C_7H_6O_9N_3Ni$, $C_{18}H_{14}O_9N_4Ni$, $C_{19}H_{14}O_{10}N_4Ni$	683	$C_{30}H_{16}O_{12}N_4Ni$, $C_{34}H_{16}O_{14}N_4Ni$, $C_{39}H_{34}O_{19}N_4Ni$ $C_{44}H_{39}O_{20}N_4Ni$
	335		762	
	488		920	
	516		1000	
((HL)$_2$Cu (OAc)$_2$) .3H$_2$O (VI)	121	$C_4H_{11}O_3N$, $C_4H_{20}O_3N$, $C_5H_{24}O_5N$, $C_7H_{26}O_5N_2Cu$,	381	$C_{14}H_{26}O_6N_2Cu$, $C_{25}H_{28}O_{12}N_2Cu$, $C_{36}H_{34}O_{18}N_2Cu$, $C_{42}H_{42}O_{20}N_4Cu$ $C_{45}H_{42}O_{20}N_4Cu$
	130		611	
	178		845	
	281		986	
			1021	
(((HL)$_2$Zn (SO$_4$) (H$_2$O)) .2H$_2$O (VII)	671	$C_{22}H_{28}O_{15}N_3SZn$, $C_{24}H_{28}O_{15}N_3SZn$, $C_{27}H_{28}O_{15}N_4SZn$, $C_{35}H_{32}O_{15}N_4SZn$,	890	$C_{36}H_{33}O_{17}N_4SZn$, $C_{40}H_{34}O_{18}N_4SZn$ $C_{40}H_{34}O_{21}N_4SZn$
	695		955	
	744		\1002	
	845			
((HL)Ca(OAc)2 (H2O)2).3H2O (VIII)	477	$C_{18}HO_{12}N_2Ca$, $C_{18}H_4O_{12}N_2Ca$, $C_{19}H_7O_{12}N_2Ca$, $C_{20}H_8O_{13}N_2Ca$, $C_{20}H_{15}O_{13}N_2Ca$	544	$C_{21}H_{16}O_{13}N_2Ca$, $C_{23}H_{19}O_{13}N_2Ca$, $C_{23}H_{21}O_{14}N_2Ca$, $C_{23}H_{26}O_{14}N_2Ca$ $C_{24}H_{26}O_{15}N_2Ca$
	480		571	
	495		589	
	524		594	
	531		606	
((HL)Ca (Cl)$_2$ (H$_2$O)$_2$) .2H$_2$O (IX)	102	$C_3H_4O_3N$, $C_9H_{11}O_5N$, $C_{12}H_{17}O_7N_2$, $C_{18}H_{17}O_7N_2$,	454	$C_{20}H_{18}O_8N_2Ca$, $C_{20}H_{23}O_9N_2Ca$ $C_{21}H_{24}O_{10}N_2Cl_2Ca$
	213		475	
	301		575	
	413			
((HL)Pb (SO$_4$) (H$_2$O)$_3$).2H2O (X)	365	$C_5H_4O_3NSPb$, $C_6H_6O_4NSPb$, $C_9H_6O_4N_2SPb$, $C_9H_{10}O_{10}N_2SPb$	596	$C_{13}H_{13}O_{10}N_2SPb$, $C_{14}H_{17}O_{12}N_2SPb$, $C_{18}H_{22}O_{15}N_2SPb$ $C_{20}H_{22}O_{15}N_2SPb$
	394,		644	
	445		745	
	545		769	

Based on the above mentioned analytical and physical techniques, the mode of bonding and structure of the prepared complexes can be formulated (Figure 7).
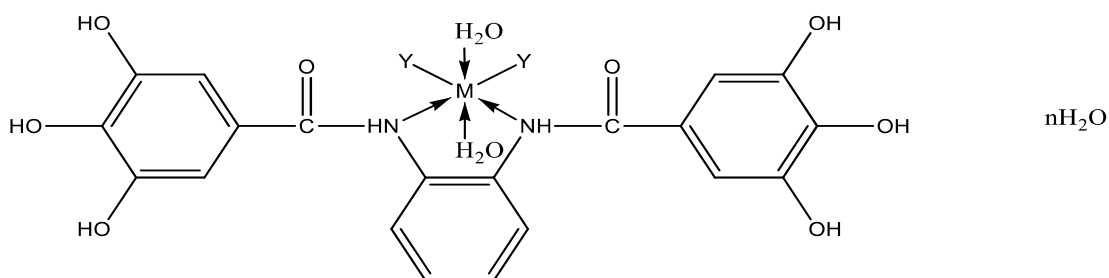

Figure 7: The mode of bonding and structure of the prepared complexes.

Electron Spin Resonance (ESR)

The ESR spectra for the two copper complexes (III), and (IV) were measured and their spectral data are presented in Table 6. The spectra are characteristic for those of d^9 configuration having axial type of a $d_{(x2-y2)}$ ground state which is the most common for Cu (II) complexes [27]. The complexes showed $g_∥>g_⊥>2.0023$, indicating octahedral geometry around Cu (II) ion [28]. The G values of the complexes are 2.75 and 3.80 i.e G<4.0 indicating that spin-exchange interactions took place between Cu (II) ions [29]. This phenomenon is further confirmed by the magnetic moments values (1.45 and 1.65 B.M.). On the other hand, the ratio of $g_∥/A_∥$ value is also considered as a diagnostic term for stereochemistry [30]. The $g_∥/A_∥$ values for the copper complexes are 170.8 and 223 cm^{-1} which lie just within the range expected for the tetragonal distorted octahedral Cu(II)complexes. The values of $α^2$ (Cu) for the two complexes calculated as: $α^2$ (Cu) = $(A_∥/0.036) + (g_∥-2.002) + 3/7 (g-2.002) + 0.04$ are 0.6 and 0.58 suggesting a covalent bonding [31].

Table 6: ESR data for Cu^{2+} complexes.

Complex	$g_∥$	$g_⊥$	g_{iso} [a]	$A_∥$ (G)	$A_⊥$ (G)	A_{iso} [b] (G)	G [c]	$g_∥/A_∥$	$α^2$	$β^2$
(III)	2.22	2.08	2.03	115	10	45	2.75	170.8	0.61	1.65
(IV)	2.23	2.06	2.12	95	5	35	3.8	223	0.58	1.34

Transmission Electron Microscopy (TEM)

Study of the TEM images of some selected complexes reveals that the average diameter of particles sizes ranges from 43 to 58 nm that are lying in the nano-sized range. Illustrative example is shown in Figure 8 for Cu complex (III) (Figure 8).

Antimicrobial activity assay

The antimicrobial profile was tested against two Gram positive bacterial species (*Staphylococcus aureus*, (*Staph. Aureus*) and *Bacillus subtilis*, (*Bacillus subtilis*)), two Gram negative bacterial species (*Escherichia coli, (Escherichia*

Citation: Moustafa IMI, et al. 2024. N, N'-(1,2-Pheneylene) bis (3,4,5-Trihudroxybenzamide) as Bioactive Ligand; Synthesis, Analytical and Anti-Microbial Studies. J. Chem Pharm. Res. 16:170.

Moustafa IMI, et al.   *J. Chem. Pharm. Res., 2024, 16(7):1-16*

coli), *Proteus vulgaris*), one filamentous fungus (*Aspergillus fumigatus*, (*Asp. fumigatus*)) and one yeast species (*Candida albicans*, (*Cand. albicans*)) using a modified well diffusion method. The resulting inhibition zone diameters were measured in millimeters and used as criterion for the antimicrobial activity with addition to the % Activity Index.
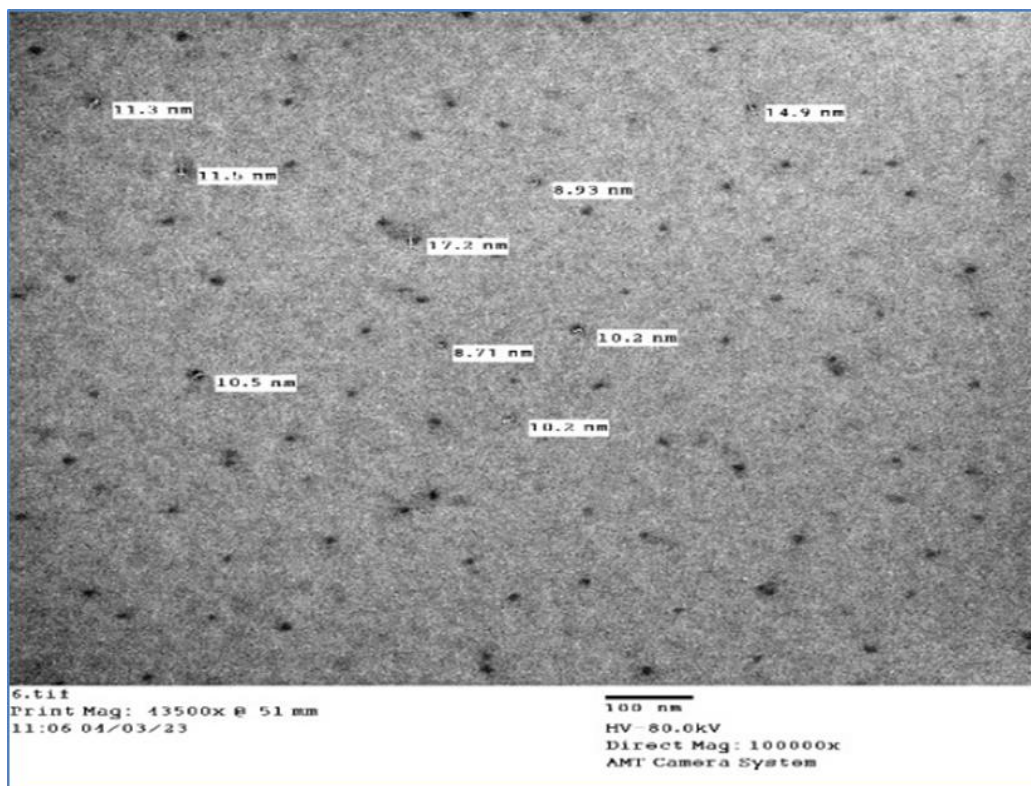

Figure 8: TEM images for Cu Complex (III).

DMSO, used for dissolving the test compounds, was included in every experiment as negative controls and showed no inhibition zones. Positive controls were also performed using gentamycin as standard antibacterial drugs (4 µg/ml) and ketoconazole as standard antifungal drug (100 µg/ml). The antibacterial and antifungal results (Table 7) showed that the organic free ligand showed high activity towards the tested organism compared to the positive controls used as standard drugs and most of the complexes exhibit higher activities than the free ligand except for the Gram positive bacteria, *Staph. Aureus*, where the solid complexes showed less activity than the organic ligand. The increased activity of metal complexes is explained by the overtone's concept and the Tweedy's theory according to which chelation reduces the polarity of the ligand due to partial sharing of its negative charge with the metal favouring the transportation of the complex across the lipid layer of the cell membrane. On the other hand, the negative results observed in some cases can be attributed to the inability of the complex to diffuse into bacterial cell membranes or it can diffuse by inactivited rout by any cellular mechanism [32-35]. The test was done using the diffusion agar technique, well diameter: 6.0 mm (100 µl was tested), at RCMB: Regional Center for Mycology and Biotechnology.

- Positive control for fungi: Ketoconazole 100 µg/ml.

- Positive control for bacteria: Gentamycin 4 µg/ml.

- % Activity index (%Ac. Ind.) = (inhibition zone of sample/inhibition zone of control) × 100.

- *NA: No activity.

- The sample was tested in 20 mg/ml concentration.

Table 7: Antibacterial activities of studied ligand and its tested complexes in terms of inhibition zone diameter (mm) and % activity index.

Com.	*Staph. aureus*		*Bacillus subtilis*		*Escherichia coli*		*Proteus vulgaris*		*Asp.fumigatus*		*Cand. albicans*	
	Inh. zone	% Ac.Ind	Inh. Zone	% Ac.Ind	Inh. zone	% Ac.Ind	Inh. Zone	% Ac.Ind	Inh. zone	% Ac.Ind	Inh. Zone	% Ac.Ind
HL	21	87.5	13	50	12	40	18	72	14	82.4	10	50
2	16	66.7	15	57.7	18	60	18	72	15	88.2	12	60
3	9	37.5	17	65.4	12	40	22	88	17	100	14	70
4	13	54.2	20	76.9	NA	NA	12	48	17	100	14	70
5	15	62.5	19	73.1	12	40	18	72			12	60
6	17	70.8	15	57.7	11	36.7	17	68	20	117.6	NA	
7	15	62.5	17	65.4	15	50	20		NA		NA	
8	14	58.3	12	46.2	12	40	17	68	NA		NA	
9	16	66.7	20	76.9	15	50	22		16	94.1	NA	
10	10	41.7	22	84.6	12	40	NA	NA	13	76.5	NA	
11	12	50	23	88.5	18	60	21		16	94.1	18	90
	Gentamycin (4mg/ml)				Gentamycin (4mg/ml)				Ketoconazole (100mg/ml)			
	24	100	26	100	30	100	25	100	17	100	20	100

CONCLUSION

Some metal complexes of transition and non-transitiono metal ions with new polyhydroxyl amide ligand derived from Gallic acid *viz*: N, N'-(1,2-phenylene) bis (3,4,5-trihydroxy benzamide, expected to have biological activity, had been synthesized and characterized by different spectroscopic and physical techniques. The stoichiometry and stability constants of some complexes were determined by electrometric techniques (conductometric and potentiometric titrations). The biological activity of the prepared complexes towards the Gram positive bacterial species; *Staphylococcus aureus and Bacillus subtilis*, Gram negative bacterial species; *Escherichia coli*, *Proteus vulgaris*, as well as one filamentous fungus (*Aspergillus fumigatus*) and one yeast species (*Candida albicans*) was studied using a modified well diffusion method. Gentamycin antibiotics (4 µg/ml) was taken as positive control for bacteria and ketoconazole antifungal (100 µg/ml) as positive control for fungi. It was found that the majority of metal complexes showed high activities compared to the free ligand except that for the Gram positive bacteria, *Staph. Aureus*, where

the solid complexes showed less activity.

REFERENCES

[1]   Kahkeshani N, Farzaei F, Fotouhi M, et al. *Iran J Basic Med Sci*. 2019;22(3):225.

[2]   Choubey S, Varughese LR, Kumar V, et al. *Pharm Pat Anal*. 2015;4(4):305-315.

[3]   Shao D, Li J, Li J, et al. *J Food Sci*. 2015;80(6):M1299-305.

[4]   Borges A, Saavedra MJ, Simões M. *Biofouling*. 2012;28(7):755-767.

[5]   Kang MS, Oh JS, Kang IC, et al. J Microbiol. 2008;46:744-750.

[6]   Teodoro GR, Ellepola K, Seneviratne CJ, et al. *Front Microbiol*. 2015;6:1420.

[7]   Oh E, Jeon B. *Front Microbiol*. 2015;6:1129.

[8]   Nohynek LJ, Alakomi HL, Kähkönen MP, et al. *Nutr Cancer*. 2006;54(1):18-32.

[9]   Omojate Godstime C, Enwa Felix O, Jewo Augustina O, et al. *J Pharm Chem Biol Sci*. 2014;2(2):77-85.

[10] Kubo I, Fujita KI, Nihei KI, et al. *Bioorg Med Chem*. 2003;11(4):573-580.

[11] Hao YN, Gao YR, Li Y, et al. *Adv Mater Interfaces*. 2021;8(24):2101173.

[12] Sumrra SH, Zafar W, Imran M, et al. *J Coord Chem*. 2022;75(3-4):293-334.

[13] Arslan M. React Funct Polym. 2019;139:9-16.

[14] Fazary AE, Taha M, Ju YH. *J Chem Eng Data*. 2009;54(1):35-42.

[15] Badhani B, Sharma N, Kakkar R. *Rsc Advances*. 2015;5(35):27540-52757.

[16] Wang X, Cong J, Zhang L, et al. *J Agric Food Chem*. 2023;71(41):15352-15362.

[17] Al-Rashdi AA, Naggar AH, Farghaly OA, et al. Am J Anal Chem. 2018;9(3):99-112.

[18] Al-Mohaimeed AM, Alothman AA. *J Chem*. 2019;2019(1):1064942.

[19] Zaid AA, Farooqui M, Janrao DM. *J Saudi Chem Soc*. 2015;19(1):92-96.

[20] Abdou S, Abd-El Wahed MM, Abu-Setta MH. *Int J Adv Chem*. 2018;4(1):17-37.

[21] Moustafa IM, Mohamed NM, Ibrahim SM. *Open J Inorg Chem*. 2022;12(3):39-56.

[22] Morrissey I, Bouchillon SK, et al. *J Med Microbiol*. 2014;63(4):556-561.

[23] Abo-Ashour MF, Eldehna WM, George RF, et al. *Eur J Med Chem*. 2018;160:49-60.

[24] Ibrahim HS, Eldehna WM, Abdel-Aziz HA, et al. *Eur J Med Chem*. 2014;85:480-486.

[25] Shahen I, Ibraheem S, El-Feky F, et al. *Egypt J Chem*. 2022;65(6):773-790.

[26] Griesar K, Haase W. *J Magn Org Chem* 2023;325-344.

[27] Pei S, You S, Ma J, et al. *Environ Sci Technol*. 2020;54(20):13333-13343.

[28] El-Tabl AS, Shaban MT, Abd El-Wahed NM. *J Chem Chem Sci*. 2019;9(3):74-108.

[29] Barba FJ, Roohinejad S, Ishikawa K, et al. *Trends Food Sci Technol*. 2020;100:77-87.

[30] Delgado F, Lorente N. *Prog. Surf. Sci*. 2021;96(2):100625.

[31] Hwang J, Krylov D, Elbertse R, et al. *Rev Sci Instrum*. 2022;93(9).

[32] Wagaw S, Buchwald SL. *J Org Chem*. 1996;61(21):7240-7241.

[33] Sompila AW, Mabika AB, Pambou-Tobi NP, et al. *Am. J. Anal. Chem*. 2021;12(12):506-519.

[34] Smith RL, Soeters MR, Wüst RC, et al. *Endocrine reviews*. 2018;39(4):489-517.

[35] Tweedy BG. *Phytopathology*. 1964;55(8):910-914.